APPLICATION OF THE MULTIPLE RECIPROCITY BEM FOR NUMERICAL SOLUTION OF BIOHEAT TRANSFER EQUATION

***Ewa Majchrzak*[1, 2], *Joanna Drozdek*[2], *Grażyna Kałuża*[1]**

[1]*Silesian University of Technology, Gliwice*
[2]*Technical University of Częstochowa, Częstochowa*

Abstract. Application of the standard boundary element method for numerical solution of the bioheat transfer equation requires discretization not only the boundary but also the interior of the domain considered. In this paper the variant of the BEM which is connected only with the boundary discretization is presented. It is the essential advantage of the algorithm proposed in comparison with the classical one. As the example, the problem of the pair of vessels (artery and vein) surrounded by the tissue is analyzed, and the temperature field in the tissue sub-domain is found.

1. Bioheat transfer equation

The blood perfusion greatly affects the thermal response of living tissue. From the mathematical point of view the problem belongs to the boundary (or boundary initial) ones and is described by the partial differential equation called the bioheat transfer equation (Pennes equation) and the boundary (or the boundary and initial) conditions [1-3].

Pennes proposed quantifying heat transfer effects in perfused biological tissue by a heat source appearing in the energy equation. The capacity of internal heat sources is proportional to the perfusion rate and the difference between the tissue teperature and the global arterial blood temperature. The underlying assumption was that all heat transfer occurs in the capillaries. The Pennes equation has the inherent limitation that is cannot simulate the effects of large, widely spaced thermally significat blood vessels and they must be treated separately [2].

In this paper we cosider the steady state problem and then the Pennes equation takes a form

$$x \in \Omega : \lambda \nabla^2 T(x) + c_B G_B \left[T_B - T(x)\right] + Q_{met} = 0 \tag{1}$$

where: λ is the thermal conductivity, W/mK, Q_{met} is the metabolic heat source, W/m^3, G_B is the blood perfusion rate, m^3/s/m^3 tissue, c_B is the volumetric specific heat of blood, J/m^3 K, T_B is the arterial blood temperature, T denotes the temperature. The 2D problem is considered, this means $x = \{x_1, x_2\}$.

The metabolic heat source, as a rule, is treated as a constant value [2], according to the environmental conditions (cold, rest, exercise).

The capacity of this component changes from 245 to 24500 W/m^3.
Equation (1) is supplemented by the boundary conditions

$$\begin{cases} x \in \Gamma_1: & T(x) = T_b \\ x \in \Gamma_2: & q(x) = -\lambda \dfrac{\partial T(x)}{\partial n} = q_b \\ x \in \Gamma_3: & q(x) = -\lambda \dfrac{\partial T(x)}{\partial n} = \alpha \, [T(x) - T^{\infty}] \end{cases} \tag{2}$$

wher $\Gamma = \Gamma_1 \cup \Gamma_2 \cup \Gamma_3$ is the boundary of the domain Ω, T_b and q_b are the known temperature and heat flux, α is the heat transfer coefficient, T^{∞} is the ambient temperature, $\partial T/\partial n$ is the normal derivative.
The equation (1) can be written in the form

$$x \in \Omega: \ \lambda \nabla^2 T(x) - k\, T(x) + Q = 0 \tag{3}$$

where

$$k = G_B \, c_B, \qquad Q = k\, T_B + Q_{met} \tag{4}$$

From the mathematical point view, equation (3) is the Poisson equation with the temperature dependent heat source function.

2. Boundary element method

The standard boundary element method algorithm leads to the following integral equation [4-6]

$$\begin{gathered} B(\xi)\, T(\xi) + \int_{\Gamma} V_0^*(\xi, x)\, q(x)\, \mathrm{d}\Gamma = \\ \int_{\Gamma} Z_0^*(\xi, x)\, T(x)\, \mathrm{d}\Gamma + \int_{\Omega} [Q - k\, T(x)]\, V_0^*(\xi, x)\, \mathrm{d}\Omega \end{gathered} \tag{5}$$

where ξ is the observation point, $B(\xi) \in (0, 1]$, $V_0^*(\xi, x)$ is the fundamental solution

$$V_0^*(\xi, x) = \frac{1}{2\pi\lambda} \ln \frac{1}{r} \tag{6}$$

r is the distance between the points ξ and x

$$r = \sqrt{(x_1 - \xi_1)^2 + (x_1 - \xi_1)^2} \tag{7}$$

while

$$Z_0^*(\xi, x) = -\lambda \frac{\partial V_0^*(\xi, x)}{\partial n} \tag{8}$$

and

$$q(x) = -\lambda \frac{\partial T(x)}{\partial n} \tag{9}$$

The heat flaux resulting from fundamental solution can be calculated analytically

$$Z_0^*(x) = \frac{d}{2 \pi r^2} \tag{10}$$

where

$$d = (x_1 - \xi_1)\cos\alpha_1 + (x_2 - \xi_2)\cos\alpha_2 \tag{11}$$

and $\cos\alpha_1$, $\cos\alpha_2$ are the directional cosinesof the normal outward vector *n*.

In numerical realization of this variant of the BEM the boundary Γ and also the interior Ω must be discretized.

3. Multiple reprocity BEM

We denote by *I* the last integral in equation (5), namely

$$I = \int_\Omega [Q - k\,T(x)]\, V_0^*(\xi, x)\, \mathrm{d}\Omega \tag{12}$$

If the function $V_1^*(\xi, x)$ fulfills the equation

$$V_0^*(\xi, x) = \nabla^2 V_1^*(\xi, x) \tag{13}$$

then using the 2nd Green formula [5] one obtains

$$\begin{gathered} I = \int_\Omega [Q - k\,T(x)]\nabla^2 V_1^*(\xi, x)\,\mathrm{d}\Omega = -k\int_\Omega \nabla^2 T(x)\, V_1^*(\xi, x)\,\mathrm{d}\Omega + \\ \int_\Gamma \left[[Q - k\,T(x)] \frac{\partial V_1^*(\xi, x)}{\partial n} + k\,V_1^*(\xi, x)\frac{\partial T(x)}{\partial n} \right] \mathrm{d}\Gamma \end{gathered} \tag{14}$$

Because (c.f. equation (3))

$$\nabla^2 T(x) = \frac{k}{\lambda} T(x) - \frac{1}{\lambda} Q \tag{15}$$

therefore

$$\begin{aligned} I = {} & \frac{k}{\lambda} \int_\Omega \left[Q - k\, T(x) \right] V_1^* (\xi, x)\, \mathrm{d}\,\Omega - \frac{Q}{\lambda} \int_\Gamma Z_1^* (\xi, x)\, \mathrm{d}\,\Gamma + \\ & \frac{k}{\lambda} \int_\Gamma Z_1^* (\xi, x)\, T(x)\, \mathrm{d}\,\Gamma - \frac{k}{\lambda} \int_\Gamma V_1^* (\xi, x)\, q(x)\, \mathrm{d}\,\Gamma \end{aligned} \tag{16}$$

where

$$Z_1^*(\xi, x) = -\lambda \frac{\partial V_1^*(\xi, x)}{\partial n} \tag{17}$$

Now, we assume that the function $V_2^*(\xi, x)$ begin the solution of equation

$$V_1^*(\xi, x) = \nabla^2 V_2^*(\xi, x) \tag{18}$$

is known and the integral

$$I_1 = \int_\Omega \left[Q - k\, T(x) \right] V_1^* (\xi, x)\, \mathrm{d}\,\Omega \tag{19}$$

can be transformed to the form

$$\begin{aligned} I_1 = {} & \frac{k}{\lambda} \int_\Omega \left[Q - k\, T(x) \right] V_2^* (\xi, x)\, \mathrm{d}\,\Omega - \frac{Q}{\lambda} \int_\Gamma Z_2^* (\xi, x)\, \mathrm{d}\,\Gamma + \\ & \frac{k}{\lambda} \int_\Gamma Z_2^* (\xi, x)\, T(x)\, \mathrm{d}\,\Gamma - \frac{k}{\lambda} \int_\Gamma V_2^* (\xi, x)\, q(x)\, \mathrm{d}\,\Gamma \end{aligned} \tag{20}$$

where

$$Z_2^*(\xi, x) = -\lambda \frac{\partial V_2^*(\xi, x)}{\partial n} \tag{21}$$

Introducing (20) into (16) one obtains

$$\begin{aligned} I = {} & \frac{k^2}{\lambda^2} \int_\Omega \left[Q - k\, T(x) \right] V_2^* (\xi, x)\, \mathrm{d}\,\Omega - \frac{Q}{\lambda} \int_\Gamma Z_1^* (\xi, x)\, \mathrm{d}\,\Gamma - \\ & Q \frac{k}{\lambda^2} \int_\Gamma Z_2^* (\xi, x)\, \mathrm{d}\,\Gamma + \frac{k}{\lambda} \int_\Gamma Z_1^* (\xi, x)\, T(x)\, \mathrm{d}\,\Gamma + \frac{k^2}{\lambda^2} \int_\Gamma Z_2^* (\xi, x)\, \mathrm{d}\,\Gamma - \\ & \frac{k}{\lambda} \int_\Gamma V_1^* (\xi, x)\, q(x)\, \mathrm{d}\,\Gamma - \frac{k^2}{\lambda^2} \int_\Gamma V_2^* (\xi, x)\, q(x)\, \mathrm{d}\,\Gamma \end{aligned} \tag{22}$$

This procedure can be easily generalized. The following sequence of functions is defined

$$\begin{aligned} &\nabla^2 V_{l+1}^*(\xi, x) = V_l^*(\xi, x), \qquad l = 0, 1, 2, ... \\ &Z_l^*(\xi, x) = -\lambda \frac{\partial V_l^*(\xi, x)}{\partial n} \end{aligned} \tag{23}$$

and then the integral equation (5) can be written in the form

$$\begin{aligned} &B(\xi)\, T(\xi) + \sum_{l=0}^{\infty} \left(\frac{k}{\lambda} \right)^l \int_\Gamma V_l^*(\xi, x)\, q(x)\, \mathrm{d}\,\Gamma = \\ &\sum_{l=0}^{\infty} \left(\frac{k}{\lambda} \right)^l \int_\Gamma Z_l^*(\xi, x)\, T(x)\, \mathrm{d}\,\Gamma - \frac{Q}{\lambda} \sum_{l=0}^{\infty} \left(\frac{k}{\lambda} \right)^l \int_\Gamma Z_{l+1}^*(\xi, x)\, \mathrm{d}\,\Gamma \end{aligned} \tag{24}$$

This equation contains only the boundary integrals. In order to solve it, the functions $V_l^*(\xi, x)$ must be known and the adequate series must be convergent [6]. In [6] the following formulas are presented

$$V_l^*(\xi, x) = \frac{1}{2\pi\lambda} r^{2l} \left(A_l \ln \frac{1}{r} + B_l \right), \qquad l = 0, 1, 1, \ldots \tag{25}$$

where

$$\begin{aligned} &A_0 = 1, \;\; A_{l+1} = \frac{A_l}{4\left(l+1\right)^2}, \qquad l = 0, 1, 2, \ldots \\ &B_0 = 0, \;\; B_{l+1} = \frac{1}{4\,(l+1)^2} \left(\frac{A_l}{l+1} + B_l \right), \qquad l = 0, 1, 2, \ldots \end{aligned} \tag{26}$$

The functions $Z_l^*(\xi, x)$ can be calculated in the analytic way (c.f. equations (23))

$$Z_l^*(\xi, x) = \frac{d}{2\pi} r^{2l-2} \left[A_l - 2\,l \left(A_l \ln \frac{1}{r} + B_l \right) \right] \tag{27}$$

4. Numerical model

The boundary is divided into N boundary elements Γ_j, $j = 1, 2, \ldots, N$. The integrals in equation (24) are substituted by the sums of integrals over these elements

$$B(\xi^i)\,T(\xi^i)+\sum_{l=0}^{\infty}\left(\frac{k}{\lambda}\right)^l\sum_{j=1}^{N}\int\limits_{\Gamma_j} q(x)\,V_l^*(\xi^i,x)\,\mathrm{d}\,\Gamma_j =$$
$$\sum_{l=0}^{\infty}\left(\frac{k}{\lambda}\right)^l\sum_{j=1}^{N}\int\limits_{\Gamma_j} T(x)\,Z_l^*(\xi^i,x)\,\mathrm{d}\,\Gamma_j-\frac{Q}{\lambda}\sum_{l=0}^{\infty}\left(\frac{k}{\lambda}\right)^l\sum_{j=1}^{N}\int\limits_{\Gamma_j} Z_{l+1}^*(\xi^i,x)\,\mathrm{d}\,\Gamma_j \tag{28}$$

If the parabolic boundary elements are used [4-6] then (Fig. 1)

$$x=(x_1,x_2)\in\Gamma_j:\ \begin{cases} x_1=N_p\,x_1^p+N_s\,x_1^s+N_k\,x_1^k \\ x_2=N_p\,x_2^p+N_s\,x_2^s+N_k\,x_2^k \end{cases} \tag{29}$$

and

$$x\in\Gamma_j:\ \begin{cases} T=N_p\,T_p+N_s\,T_s+N_k\,T_k \\ q=N_p\,q_p+N_s\,q_s+N_k\,q_k \end{cases} \tag{30}$$

where

$$N_p=\frac{\eta\,(\eta-1)}{2},\qquad N_s=(1+\eta)(1-\eta),\qquad N_k=\frac{\eta\,(\eta+1)}{2} \tag{31}$$

while $\eta\in[-1,1]$.

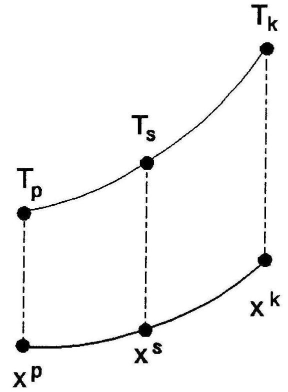

Fig. 1. Parabolic boundary element

Because

$$\mathrm{d}\,\Gamma_j=\sqrt{\left(\frac{\mathrm{d}\,x_1}{\mathrm{d}\,\eta}\right)^2+\left(\frac{\mathrm{d}\,x_2}{\mathrm{d}\,\eta}\right)^2}\,\mathrm{d}\,\eta \tag{32}$$

so

$$\mathrm{d}\,\Gamma_j = f\,(\eta)\,\mathrm{d}\,\eta = \sqrt{\left(\frac{2\,\eta-1}{2}\,x_1^p - 2\,\eta\,x_1^s + \frac{2\,\eta+1}{2}\,x_1^k\right)^2 + \left(\frac{2\,\eta-1}{2}\,x_2^p - 2\,\eta\,x_2^s + \frac{2\,\eta+1}{2}\,x_2^k\right)^2}\,\mathrm{d}\,\eta \tag{33}$$

The integrals appearing in equation (28) can be written in the form

$$\int_{\Gamma_j} q(x)\,V_l^*(\xi^i, x)\,\mathrm{d}\,\Gamma_j = g_{ij}^{pl}\,q_p + g_{ij}^{sl}\,q_s + g_{ij}^{kl}\,q_k \tag{34}$$

and

$$\int_{\Gamma_j} T(x)\,Z_l^*(\xi^i, x)\,\mathrm{d}\,\Gamma_j = h_{ij}^{pl}\,T_p + h_{ij}^{sl}\,T_s + h_{ij}^{kl}\,T_k \tag{35}$$

while

$$\int_{\Gamma_j} Z_{l+1}^*(\xi^i, x)\,\mathrm{d}\,\Gamma_j = h_{ij}^{p\,l+1} + h_{ij}^{s\,l+1} + h_{ij}^{k\,l+1} \tag{36}$$

where

$$g_{ij}^{pl} = \int_{-1}^{1} N_p\,V_l^*\left(\xi_1^*, \xi_2^i,\; N_p\,x_1^p + N_s\,x_1^s + N_k\,x_1^k,\; N_p\,x_2^p + N_s\,x_2^s + N_k\,x_2^k\right) f(\eta)\,\mathrm{d}\,\eta \tag{37}$$

$$g_{ij}^{sl} = \int_{-1}^{1} N_s\,V_l^*\left(\xi_1^*, \xi_2^i,\; N_p\,x_1^p + N_s\,x_1^s + N_k\,x_1^k,\; N_p\,x_2^p + N_s\,x_2^s + N_k\,x_2^k\right) f(\eta)\,\mathrm{d}\,\eta \tag{38}$$

$$g_{ij}^{kl} = \int_{-1}^{1} N_k\,V_l^*\left(\xi_1^*, \xi_2^i,\; N_p\,x_1^p + N_s\,x_1^s + N_k\,x_1^k,\; N_p\,x_2^p + N_s\,x_2^s + N_k\,x_2^k\right) f(\eta)\,\mathrm{d}\,\eta \tag{39}$$

and

$$h_{ij}^{pl} = \int_{-1}^{1} N_p\,Z_l^*\left(\xi_1^*, \xi_2^i,\; N_p\,x_1^p + N_s\,x_1^s + N_k\,x_1^k,\; N_p\,x_2^p + N_s\,x_2^s + N_k\,x_2^k\right) f(\eta)\,\mathrm{d}\,\eta \tag{40}$$

$$h_{ij}^{sl} =$$

$$\int_{-1}^{1} N_s Z_l^* \left(\xi_1^*, \xi_2^i, N_p x_1^p + N_s x_1^s + N_k x_1^k, N_p x_2^p + N_s x_2^s + N_k x_2^k \right) f(\eta)\, \mathrm{d}\eta \tag{41}$$

$$h_{ij}^{kl} =$$

$$\int_{-1}^{1} N_k Z_l^* \left(\xi_1^*, \xi_2^i, N_p x_1^p + N_s x_1^s + N_k x_1^k, N_p x_2^p + N_s x_2^s + N_k x_2^k \right) f(\eta)\, \mathrm{d}\eta \tag{42}$$

As well known, in the final system of algebraic equations the values of temperatures or heat fluxes are connected with the boundary nodes. If the following numeration of the bounary nodes r = 1, 2,..., R is accepted then for i = 1, 2,..., R one obtains the system of equations (c.f. equation (28))

$$B_i T_i + \sum_{l=0}^{\infty} \left(\frac{k}{\lambda} \right)^l \sum_{r=1}^{R} g_{ir}^l q_r = \sum_{l=0}^{\infty} \left(\frac{k}{\lambda} \right)^l \sum_{r=1}^{R} h_{ir}^l T_r - \frac{Q}{\lambda} \sum_{l=0}^{\infty} \left(\frac{k}{\lambda} \right)^l \sum_{r=1}^{R} h_{ir}^{l+1} \tag{43}$$

where for single node r begin the end of the boundary element Γ_j and begin the beginning of the boundary element Γ_{j+1} we have:

$$\begin{aligned} g_{ir}^l &= g_{i,j}^{kl} + g_{i,j+1}^{pl} \\ h_{ir}^l &= h_{i,j}^{kl} + h_{i,j+1}^{pl} \end{aligned} \tag{44}$$

for double node r, r + 1:

$$\begin{aligned} g_{ir}^l &= g_{i,j}^{kl}, \qquad g_{i,r+1}^l = g_{i,j+1}^{pl} \\ h_{ir}^l &= h_{i,j}^{kl}, \qquad h_{i,r+1}^l = h_{i,j+1}^{pl} \end{aligned} \tag{45}$$

while for the central node r of the boundary element Γ_j:

$$g_{ir}^l = g_{ij}^{sl}, \qquad h_{ir}^l = h_{ij}^{sl} \tag{46}$$

The system of equations (43) can be written in the form

$$\sum_{r=1}^{R} G_{ir} q_r = \sum_{r=1}^{R} H_{ir} T_r + \sum_{r=1}^{R} Z_{ir}, \qquad i = 1, 2, \ldots, R \tag{47}$$

where:

$$G_{ir} = \sum_{l=0}^{\infty} \left(\frac{k}{\lambda} \right)^{l} g_{ir}^{l} \tag{48}$$

$$H_{ir} = \sum_{l=0}^{\infty} \left(\frac{k}{\lambda} \right)^{l} h_{ir}^{l}, \quad i \neq r \tag{49}$$

$$H_{ii} = -\sum_{\substack{r=1 \\ r \neq i}}^{R} H_{ir}, \quad i = r \tag{50}$$

$$Z_{ir} = -\frac{Q}{\lambda} \sum_{l=0}^{\infty} \left(\frac{k}{\lambda} \right)^{l} h_{ir}^{l+1} \tag{51}$$

Taking into account the boundary conditions (2) the system of equations must be rebuilt to the form **A Y = F**. The solution of this system allows to determine the „missing" boundary temperatures and heat fluxes. Next, the temperatures at optional sat of internal nodes can be calculated using the formula

$$T_i = \sum_{r=1}^{R} H_{ir} T_r - \sum_{r=1}^{R} G_{ir} q_r + \sum_{r=1}^{R} Z_{ir} \tag{52}$$

5. Example of computations

The pair of blood vessels (artery and vein) surrounded by the tissue is analyzed - Figure 2. The domain considered corresponds to the cross-sectional area of the tissue cylinder - Figure 3. Its radius R is equal to the inverse of the vessel pair density and this Krogh-type tissue cylinder is affected only by the blood vessels pair which is located in the central part of the domain.

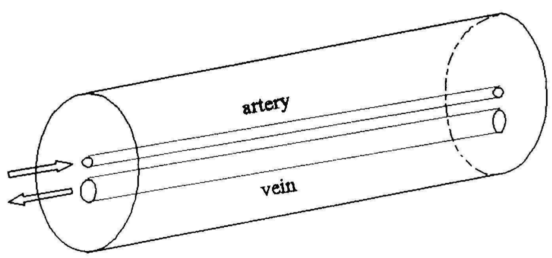

Fig. 2. Pair of blood vessels

Radius of artery equals $R_1 = 0.0002$ m, radius of vein $R_2 = 0.0003$ m, radius of t tissue cylinder $R = 0.0015$ m, distance between the blood vassels $D = 0.0003$ m (c.f. Figure 3).

The following boundary conditions have been accepted:

$$
\begin{aligned}
x \in \Gamma_1: &\quad q(x) = -\lambda \frac{\partial T(x)}{\partial n} = \alpha_1 [T(x) - T_{B1}] \\
x \in \Gamma_2: &\quad q(x) = -\lambda \frac{\partial T(x)}{\partial n} = \alpha_2 [T(x) - T_{B2}] \\
x \in \Gamma_0: &\quad q(x) = -\lambda \frac{\partial T(x)}{\partial n} = 0
\end{aligned}
\tag{53}
$$

Assuming that for artery and vein the Nusselt number Nu = 4 [1, 2] one obtains $\alpha_1 = 5000$ W/m$^2 \cdot$ K, $\alpha_2 = 3333.33$ W/m$^2 \cdot$ K. Thermal conductivity of tissue equals $\lambda = 0.5$ W/mK, the blood temperatures: $T_B = 37.5$°C (arterial) $T_{B1} = 37.33$°C (artery), $T_{B2} = 37$°C (vein),volumetric specific heat of blood $c_B = 3.9962 \cdot 10^6$ J/m^{3}K. The remaining data are following: perfusion coefficient $G_B = 0.0005425$ m^3/s/m^3 tissue, metabolic heat source $Q_{met} = 245$ W/m^3 for rest conditions, while $G_B =$ $= 0.01085$ m^3/s/m^3 tissue, $Q_{met} = 24500$ W/m^3 for exercise conditions [1].

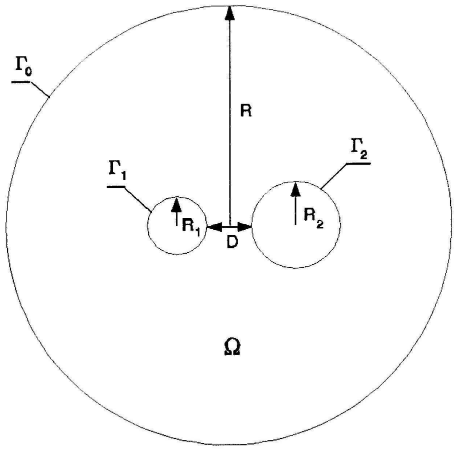

Fig. 3. Cross-section of tissue cylinder

The external boundary is divided into 60 parabolic boundary elements (120 nodes), while the internal boundaries are divided into 8 (16 nodes) and 12 (24 nodes) parabolic boundary elements for artery and vein, respectively - Figure 4. In Figure 4 the position of internal nodes is also marked.

The same problem has been solved by Mochnacki and Majchrzak [7] using the classical boundary element algorithm and the results obtained are practically the same. Summing up, the multiple reciprosity BEM is the effective method of numerical solution of the bioheat transfer equation.

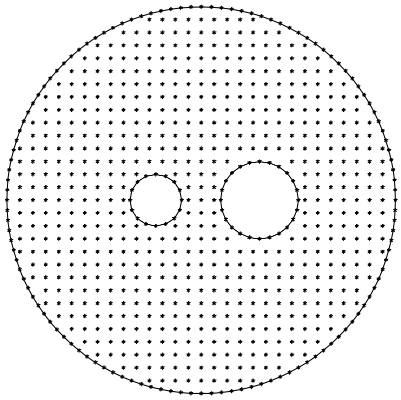

Fig. 4. Boundary discretization and internal nodes

In Figures 5 and 6 the temperature distribution in the tissue domain is shown.

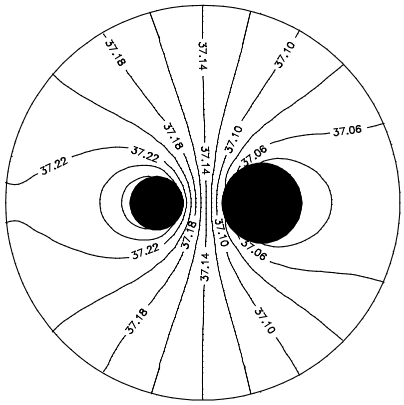

Fig. 5. Temperature distribution (rest conditions)

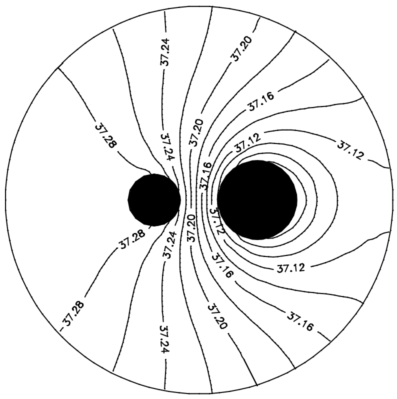

Fig. 6. Temperature distribution (execise conditions)

Acknowledgment

This research work has been supported by KBN (Grant No 8 T11F 004 19).

References

[1] Brinck H., Werner J., Estimation of the thermal effect of blood flow in a branching countercurrent network using a three-dimensional vascular model, Journal of Biomechanical Engineering 1994, 116, 324-330.

[2] Huang H.W., Chen C.L., Roemer R.B., Analytical solutions of Pennes bio-heat transfer equation with a blood vessel, Journal of Biomechanical Engineering 1994, 116, 208-212.

[3] Huang H.W., Chen Z.P., Roemer R.B., A counter current vascular network model of heat transfer in tissue, Journal of Biomechanical Engineering 1996, 118, 120-128.

[4] Brebbia C.A., Domingues J., Boundry elements, an introductory course, Computational Mechanics Publications, McGraw-Hill Book Company, London 1992.

[5] Majchrzak E., Boundary element method in the heat transfer, Publ. of the Techn. Univ. of Czest., Czestochowa 2001.

[6] Nowak A.J., Boundary element method with an application of the multiple reciprocity method, Publ. of the Sil. Univ. of Techn., 116, Gliwice 1993.

[7] Mochnacki B., Majchrzak E., Numerical solution of bio-heat transfer equation usin the boundary element method, European Congress on Computational Methods in Applied Sciences and Engineering, ECCOMAS 2000, Barcelona, 11-14 September 2000, CD-Rom Proceedings, 1-10.